Research Article   **Open Access**

Shoujian Song, Changchun Hao*, Xianggang Zhang, Qing Zhang, Runguang Sun*

Sonocatalytic degradation of methyl orange in aqueous solution using Fe-doped TiO$_2$ nanoparticles under mechanical agitation

Abstract: In the present study, the Fe-doped TiO$_2$ modified nanoparticles was successfully synthesized by the combination of the sol-gel method and heat treatment, and the degradation of methyl orange was tested by the combination method of ultrasonic radiation and mechanical agitation. The effects of different factors on the degradation of methyl orange (MO) solution were studied, such as ultrasonic irradiation time, the ultrasonic frequency, the added amount of catalyst, the initial pH value, the initial concentration of methyl orange, and revolutions per minute. The optimal experimental conditions for sonocatalytic degradation of the MO obtained were: ultrasonic irradiation time = 60 min, pH value = 3.0 and revolutions per minute = 500 rpm. By means of response surface analysis, the best fitting conditions were as follows: ultrasonic frequency = 36.02 kHz, added amount of catalyst = 490.50 mg/L, the initial concentration of methyl orange = 9.22 mg/L, and the optimum condition was close to the experimental data by response surface method. Under optimal conditions, the sonocatalytic degradation of MO was 99%. The degradation of MO showed that the combination of Fe-doped modified TiO$_2$ nanoparticles, mechanical agitation and ultrasonic irradiation was discovered that can degrade methyl orange effectively in aqueous solution.

Keywords: Sol-gel method; Sonocatalytic degradation; Fe-doped TiO$_2$ catalyst; Methyl orange; Mechanical agitation.

1 Introduction

In recent years, with the rapid development of industry, the wastewater produced has increased rapidly, while the increased wastewater threatens the freshwater resources of the human being, and becomes the environmental problem that human beings have to solve. And thus, more and more people are getting interested in the development of an effective wastewater treatment technology, in particular, the toxic carcinogenic organic dyes and pigments emitted by the textile industry have a great impact on aquatic ecosystems and human health [1-3]. Understanding the seriousness of these problems, people began to use a variety of methods to deal with the wastewater [4-8]. Organic dyes are very difficult to be decomposed of by bio-enzyme degradation and chemical oxidation degradation technology due to the steady configuration.

With the development of ultrasonic cavitation degradation, the ultrasonic catalytic degradation method has been widely used in wastewater treatment because of its many excellent properties, such as simple equipment, high efficiency, stable operation, safety and no secondary pollution [9-11]. However, in some cases, ultrasonic degradation requires a longer treatment time. Therefore, the degradation process consumes a large amount of energy [12-14]. The ultrasonic catalysis process can be improved by using a suitable catalyst, known as a sonocatalyst [4,12]. Many kinds of catalysts have been studied, including FeCeOx [15], Gd-doped CdSe [16], Bi$_2$WO$_6$ [17], Pr-doped ZnO [18], etc. In this study, modified titanium dioxide was used as the catalyst to compare the degradation efficiency of it with unmodified titanium dioxide (TiO$_2$). Making full use of the advantages of titanium dioxide as catalyst, such as good stability, cheap, no chemical toxicity and the like [4,19-21]. Previous studies on the modified Fe-doped TiO$_2$ show that iron ions are doped to titanium dioxide reduce the width of the band gap, meanwhile, the addition of iron ions retards the recombination of electrons (e$^-$) and holes (h$^+$) [22].

*Corresponding author: Changchun Hao, Runguang Sun, School of Physics and Information Technology, Shaanxi Normal University, Xi'an 710062, China, E-mail: biophymed@snnu.edu.cn
Shoujian Song, Xianggang Zhang, Qing Zhang: School of Physics and Information Technology, Shaanxi Normal University, Xi'an 710062, China

In the research, Fe-doped modified TiO_2 and pure TiO_2 were obtained by the sol-gel method and heat treatment method [23-25]. Then the structure of the obtained nanoparticles was characterized by SEM, EDS and XRD. Using the obtained nanoparticles as a catalyst for the ultrasonic degradation of organic dyes (The simulated dye is methyl orange). The effect of different factors on the degradation efficiency is studied. The influencing factors are as follows: initial amount of catalyst, the initial methyl orange concentration, the initial pH value, ultrasonic irradiation time of duration, revolutions per minute and ultrasonic radiation frequency. Additionally, considering the practical application of ultrasonic degradation of wastewater, it will be carried out in flowing liquid. This study simulated the actual situation by adding mechanical agitation to make the solution have a certain velocity, and studied its effect on the degradation.
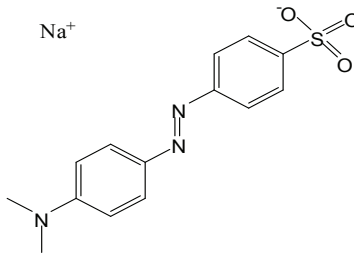
2 Experimental

2.1 Materials and methods

All the experimental reagents in the experiment were analytical grade. Tetrabutyl titanate ($C_{16}H_{36}O_4Ti$) as the titanium source, it was produced in Kemmer chemical Reagent Co, Tianjin. Ethanol (CH_3CH_2OH) was used as a reaction solution, it was produced in Kemmer chemical Reagent Co, Tianjin. Ferric nitrate nonahydrate ($FeH_{18}N_3O_{18}$) was used as the source of iron, it was produced in Tianli Chemistry Reagent Co, Tianjing. And the methyl orange ($C_{14}H_{14}N_3SO_3Na$,) was used as a simulated dye to be degraded, it was produced in Kemmer chemical Reagent Co, Tianjin, chemical structure and characteristics of the methyl orange was listed in Table 1 [26-30].

Fe-doped modified TiO_2 and pure TiO_2 nanoparticles were prepared by magnetic stirring, muffle furnace and drying furnace and the microstructural differences of the prepared nanoparticles were detected by FE-SEM (field emission scanning electron micros, Nova NanoSEM 450, FEI). The chemical composition of the prepared nanoparticles was examined by EDS (energy dispersive X-ray spectroscopy, FEI Tecnai G2 F20). After that, the crystal structure of the prepared nanoparticles was judged by XRD (X-ray diffractometry, Rigaku, Japan). The ultrasonic cleaning machine (SB-5200, Ningbo Scientz Biotechnology Co. Ltd., China) was used as a radiant point for ultrasonic experiments. The degradation of simulated organic dye methyl orange was detected by the ultraviolet spectrophotometer (UV1901PC, Shanghai Austria Science Apparatus Co. Ltd., China).

Table 1: Chemical structure and characteristics of methyl orange.

Structure	
λmax(nm)	463
M_w (g gmole^{-1})	327.33
Density at 20°C (g cm^{-3})	1.28
Solubility (mg L^{-1})	5×10^3
Molecular size (Å)	15.8 × 6.5 × 2.6
pKa	3.42

2.2 Preparation and characterization of Fe-doped modified TiO_2 powder

The process of preparation is as follows: First of all, tetrabutyl titanate and ethanol were mixed together ($C_{16}H_{36}O_4Ti$: CH_3CH_2OH = 1:4) and it was stirred intensely for 60 min. Then, a ferric nitrate nonahydrate solution (the atomic mass ratio of Fe: Ti= 0.25, 0.5, 0.75%) was added dropwise into the mixed solution. Meanwhile, dilute nitric acid and ammonia water were added to adjust the pH of the solution while stirring, so that precipitation was avoided (pH = 3, Time = 2 h). The mixture solution was placed at room temperature for two hours to form a gel, and the obtained gel was centrifuged and then dried at 75°C in the drying oven. Finally, products were heated to 800°C in a muffle furnace for 3 h and the obtained Fe-doped modified TiO_2 powder. In order to compare the experiments, the pure TiO_2 was also made in the same way. The XRD patterns of the pure TiO_2 powder and Fe-doped modified TiO_2 powder were determined using a D/Max2550 X-ray diffractometer (Cu Kα radiation (λ= 1.5406Å)). The obtained nanoparticles samples were scanned at a scanning speed of 8.0°/min in the range of 10-80° at 40 kV and 50 mA, respectively. Figure1 is the test result of XRD. Figure 2 shows the SEM images of Fe-doped modified TiO_2 and pure TiO_2 powder. Figure 4 is the test result of EDS.

2.3 Sonocatalytic reaction

All experiments were performed at room temperature (maintained at (20±2)°C) and output power was 300 W (1.3 W/ml of ultrasonic density). Methyl orange was dissolved in deionized water to obtain a certain concentration

of the solution (5, 10, 15, 20, 25 mg/L), and then add a certain amount of catalyst (0.25, 0.50, 0.75, 1.00, 1.25 g/L). After then, the mixture was stirred for 1 hour to achieve adsorption-desorption equilibrium. Then the experiment was carried out in the presence of stirring-ultrasonic. At

Figure 1: XRD patterns of (A) undoped TiO$_2$, (B) 0.25% Fe-doped TiO$_2$, (C) 0.5% Fe-doped TiO$_2$ and (D) 0.75% Fe-doped TiO$_2$ powder.

the end of the reaction, a small number of samples were taken from the reactor (four frequencies of 25, 40, 59, and 80 kHz) and all the floating titanium dioxide was removed by a centrifugal machine with a speed of 10,000 rpm. After that, the separated clear solution was measured using a UV–vis spectrometer. The concentration of methyl orange was determined at 506 nm. The degradation rate is defined as [20];

$$\text{Degradation rate}(\%) = 1 - \frac{C_t}{C_0} \times 100\%. \qquad (1)$$

Where, C_0 = initial methyl orange concentration (mg/L) C_t = methyl orange concentration at time t (min) (mg/L).

As previously reported, degradation of methyl orange dye molecules may cause the decolorization of methyl orange dye, and no absorption substance within the visible light spectrum was detected during the reaction. In this study, there is no total organic carbon (TOC), high performance liquid chromatography (HPLC), chemical oxygen demand (COD) or ion chromatography, because
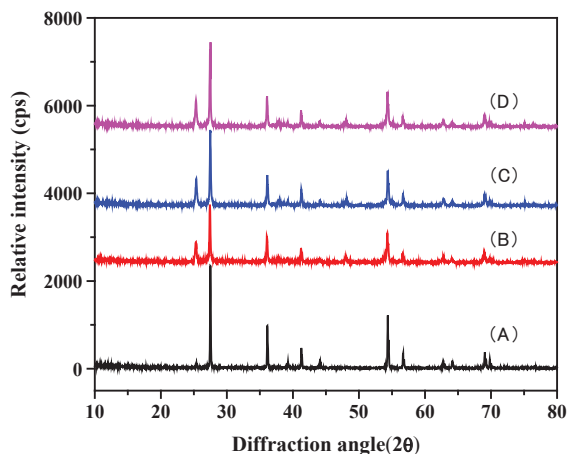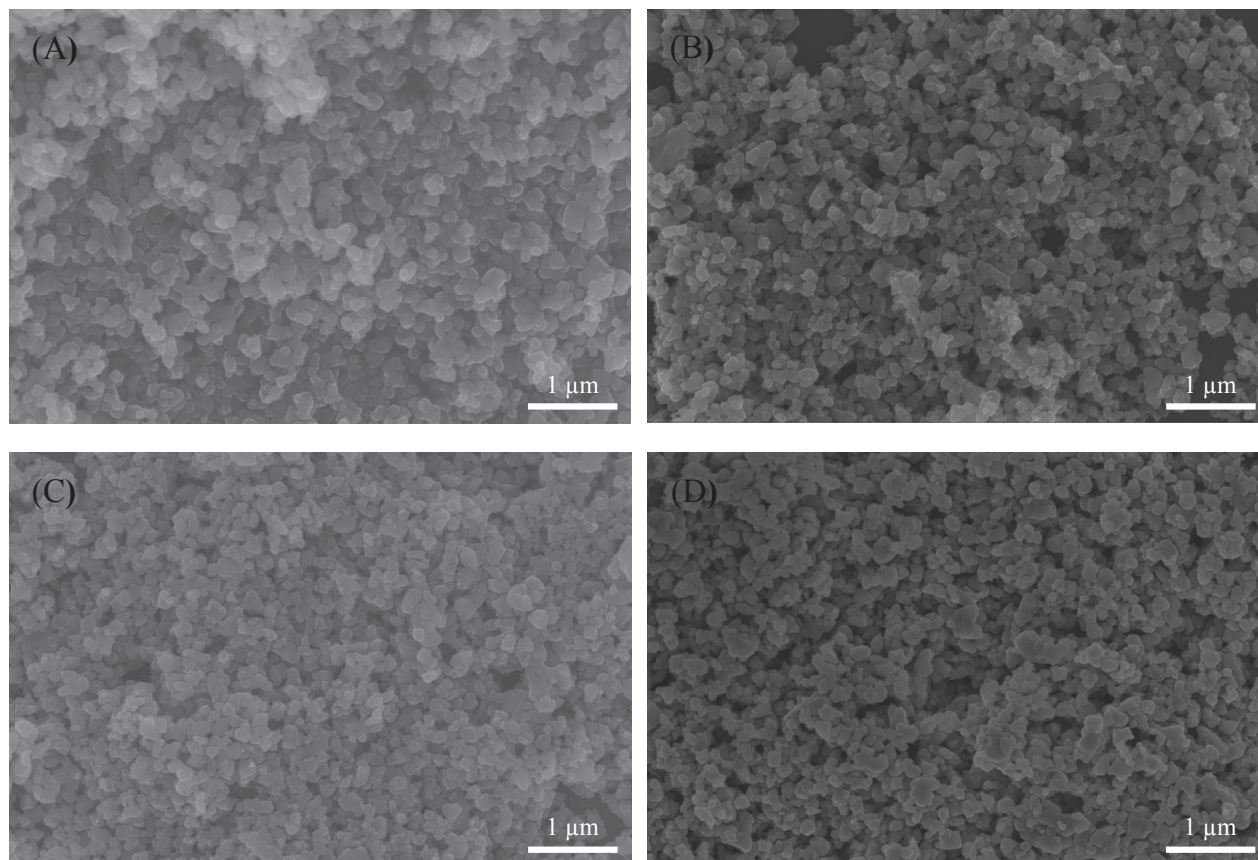

Figure 2: The SEM images of (A) undoped TiO$_2$, (B) 0.25% Fe-doped TiO$_2$, (C) 0.5% Fe-doped TiO$_2$ and (D) 0.75% Fe-doped TiO$_2$ powder.

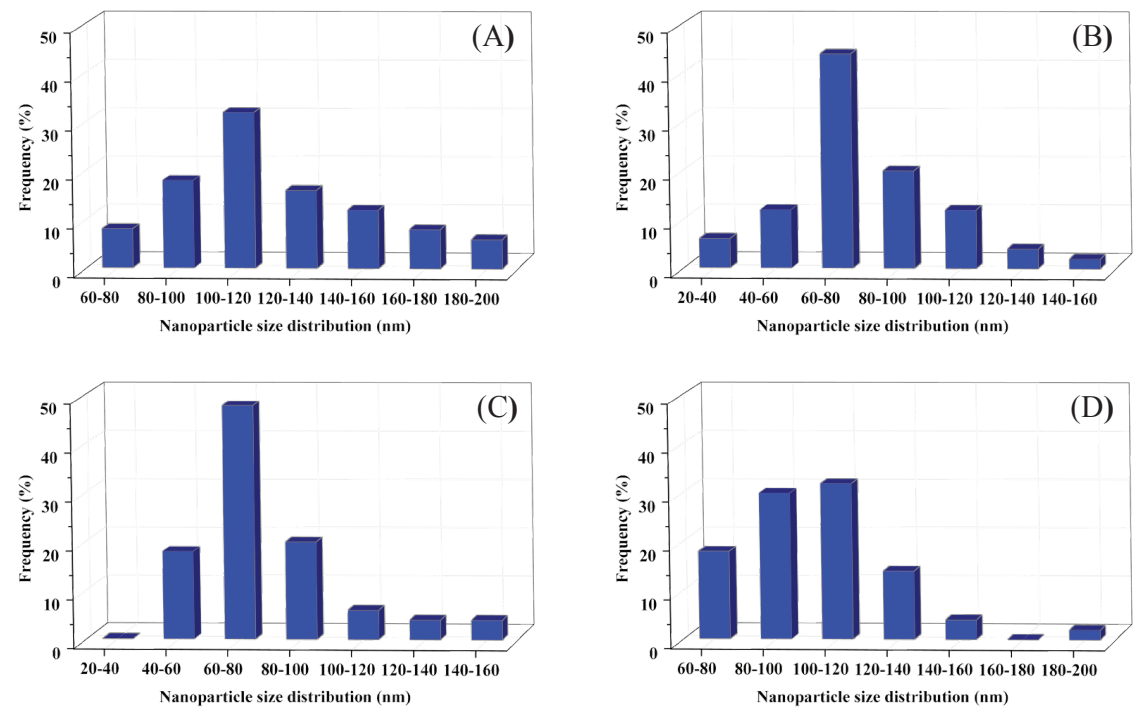**Figure 3:** The nanoparticles size distribution of (A) undoped TiO_2, (B) 0.25% Fe-doped TiO_2, (C) 0.5% Fe-doped TiO_2 and (D) 0.75% Fe-doped TiO_2 powder.
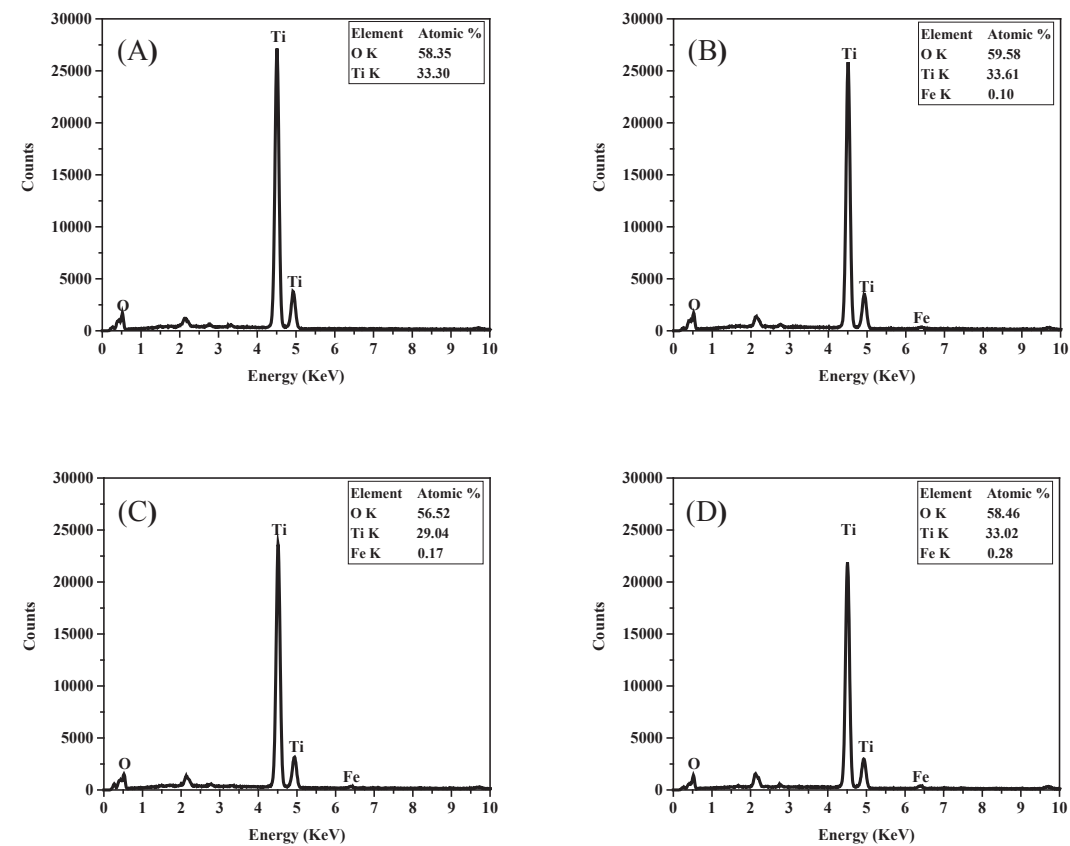

Figure 4: EDS patterns of (A) undoped TiO_2, (B) 0.25% Fe-doped TiO_2, (C) 0.5% Fe-doped TiO_2 and (D) 0.75% Fe-doped TiO_2 powder.

the scope is only to study the degradation rate of methyl orange, it is not to study the mineralization of methyl orange.

2.4 Response surface methodology

To achieve the best results, the degradation rate of organic dyes was optimized by applying the response surface method (RSM). Corresponding calculation of the experimental data was obtained by the Design Expert (version 8) software. The numerical method was employed to study the effect of different experimental condition on the degradation rate of simulated organic dye methyl orange.

Ethical approval: The conducted research is not related to either human or animal use.

3 Results and discussions

3.1 Characterization of Fe-doped modified TiO$_2$ and pure TiO$_2$ powder

3.1.1 X-ray diffraction (XRD) analysis

The influence of doping iron ions on the crystal structure of nanoparticles was detected by XRD. Figure 1 shows the XRD specimens of Fe-doped modified TiO$_2$ and pure TiO$_2$ powder. The peaks at 2θ = 25.37°, 37.91°, 48.16°, 54.05°, 55.20°, 62.87° and 75.28°,which are related to the orientations of (101), (004), (200), (105), (211), (204), and (215) planes of the anatase TiO$_2$ phase (JCPDS Card No. 73-1764). And the diffraction peaks at 2θ = 27.44°, 36.08°, 39.20°, 41.24°, 44.05°, 54.32°, 56.63°, 62.75°, 64.06°, 69.01° and 69.80°could be indexes to the (110), (101), (200), (111), (210), (211), (220), (002), (310), (301) and (112) planes of the rutile TiO$_2$ phase (JCPDS Card No. 76-0649). It can be seen that all the sample structure was made up of two different crystalline phases. In addition, no new diffraction peaks appeared, this confirms the Fe-doping onto TiO$_2$ occurred without changing the crystal structure. The average crystalline size of the TiO$_2$ nanoparticles was estimated using the Scherrer equation [32]. Mean crystalline of the undoped TiO$_2$, 0.25% Fe-doped TiO$_2$, 0.5% Fe-doped TiO$_2$ and 0.75% Fe-doped TiO$_2$ were found to be 119, 70, 69, and 106 nm, respectively. Compare these types of material of Fe-doped modified TiO$_2$ and pure TiO$_2$ powder, we can find that it has two features as follows: the diffraction peak of anatase the Fe-doped modified TiO$_2$ powder was

stronger than the corresponding the pure TiO$_2$ powder, the diffraction peak of rutile the pure TiO$_2$ powder was stronger than the corresponding the Fe-doped modified TiO$_2$ powder. According to the quantitative equation [33]:

$$\beta_A = 1/[1 + 1.26(I_R/I_A)]$$

$$\beta_R = 1/[1 + 0.8(I_A/I_R)]$$

Where, I_A, diffraction intensity of anatase (101); I_R, diffraction intensity of rutile (110), the 0.25% Fe-doped modified TiO$_2$, 0.5% Fe-doped modified TiO$_2$ and 0.75% Fe-doped modified TiO$_2$ nanoparticles includes have anatase ratio of 17.2%, 20.4% and 22.7%, respectively, and rutile ratio of 82.8%, 79.6% and 77.3%, respectively, while the pure TiO$_2$ nanoparticles have anatase ratio of 3.6% and rutile ratio of 96.4%. We can be seen that the incorporation of Fe^{3+} ions affects the structure composition of the nanoparticles. It is considered that Fe^{3+} ions as dopants hinder the transformation from the anatase phase to the rutile phase to a certain degree [33].

3.1.2 Field emission scanning electron micros (FE-SEM) analysis

The influence of iron ion incorporation on the morphology was investigated by FE-SEM measurements. Figure 2 shows SEM images of Fe-doped modified TiO$_2$ and the pure TiO$_2$ powder was produced in a spherical morphology at the nanometer scale. At the same time, it can be seen that the nanoparticles have relatively regular distribution. In the present study, the size of the nanoparticles produced at the different preparation conditions was further discussed. The grain size of four SEM images (Figure 3A to D) was statistically calculated by the nano measurement program. It was found that the size distribution of the pure TiO$_2$ powders was 80-120 nm. And the size distributions of the 0.25% Fe-doped modified TiO$_2$, 0.5% Fe-doped modified TiO$_2$ and 0.75% Fe-doped modified TiO$_2$ nanoparticles were 60-100 (43% nanoparticles were in range of 60-80), 60-100 (48% nanoparticles were in range of 60-80) and 80-120 nm, respectively. It is considered that Fe-doped modified TiO$_2$ was smaller than the corresponding pure TiO$_2$ powders, and the particle size of titanium dioxide also increases with the increase of Fe content in the sample. Therefore, the Fe-doped modified TiO$_2$ have a larger specific surface area. It can be that the addition of Fe^{3+} ions may change the way of interaction between nanoparticles and resulting in the change of the force between substances in the process of nanoparticle

formation, and the formation of smaller particles in the calcination process [32,33]. At the same time, the position of Fe^{3+} ions is different, which leads to the formation of irregular granules.

3.1.3 Energy dispersive X-ray spectroscopy (EDS) analysis

The influence of iron ion incorporation on the chemical composition was analyzed by EDS. Figure 4 shows the EDS patterns of Fe-doped modified TiO_2 and pure TiO_2 powder. The chemical composition of four EDS patterns (Figure 4A to D) were calculated, it is found that the chemical elemental contents of O and Ti have not changed greatly. At the same time, we can find that the chemical elemental content of iron was gradually increasing. The chemical elemental contents of C not shown, its can arises from conducting resin. Thus EDS results further confirmed that the incorporation of Fe^{3+} ions may affect the sizes distribution of the nanoparticles. Figure 5 shows the sonocatalytic activity of Fe-doped TiO_2 powder with different Fe^{3+} ion content. It can be seen that the Fe dopant content has no obvious effect on the degradation rate under our research conditions. Therefore, we chose 0.5% of the best amount of iron for TiO_2, because it has a larger specific surface area.

3.2 The influencing factors in sonocatalytic degradation process

3.2.1 Effect of ultrasonic irradiation time

The effect of reaction time on the degradation rate of organic dye pollutants was explored. As can be seen that the degradation effect increase with time from the Figure 6(A). During the reaction time 60 min, the color of solution changed from red to colorless. From Figure 6(B), it is found that the degradation rate of MO increases with time in three cases, including ultrasonic catalysis, ultrasound combined with Fe-doped modified titanium dioxide powder and ultrasonic combined with pure titanium dioxide powder. After 45 min, the degradation rate of Fe-doped modified titanium dioxide powder was more than 97%. Therefore, the ultrasonic radiation of 45 min is selected to continue the follow-up study. In a short period of time (within 45 minutes), it is found that the ultrasonic catalytic activity of the Fe-doped modified TiO_2 powder is greater than that of pure TiO_2 powder. We know that the addition of catalysts can accelerate the
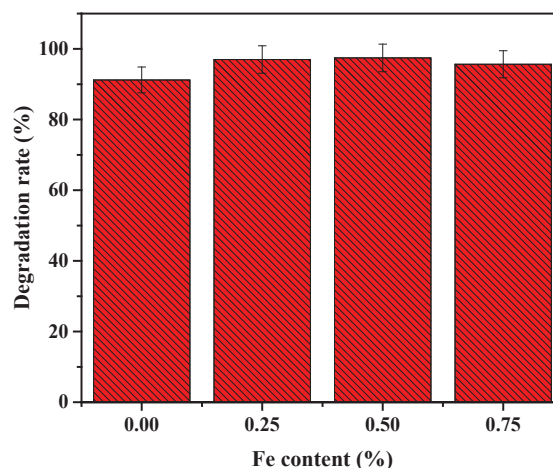

Figure 5: Effect of Fe^{3+} ion content on sonocatalytic activity of Fe-doped TiO_2 powder.

degradation of organic dyes under the same conditions. It is very important to save energy consumption in the process of degrading organic dyes.

3.2.2 Effect of ultrasonic catalyst dosage

Figure 7(A) shows a series of experimentations done by varying the loading of Fe-doped modified TiO_2 and pure TiO_2 powder from 0.25 to 1.25 g/L in order to gain the best loading. With the addition of the catalyst, the degradation rate did not show an increasing trend. The degradation rate of the simulated organic dye of methyl orange was degraded by Fe-doped modified TiO_2 powder firstly increased and then decreased, and then slightly increased with the increase of adding amount. The degradation rate of pure TiO_2 powder firstly increased and then decreased. Two different degradation effects may be attributed to a large number of nanoparticles added, resulting in the interaction between the catalysts, and then lead to the decrease of the active sites. Fe-doped modified TiO_2 was less affected, which may be related to its relatively large surface area. In conclusion, the best addition of the nanoparticle catalyst is 500 mg/L.

3.2.3 Effect of MO initial concentration

The effect of initial concentration (5, 10, 15, 20 and 25 mg/L) of the simulated organic dye of methyl orange on the degradation efficiency was studied. From Figure 7(B), it can be found that the best degradation concentration of simulated organic dye of methyl orange was 10 mg/L
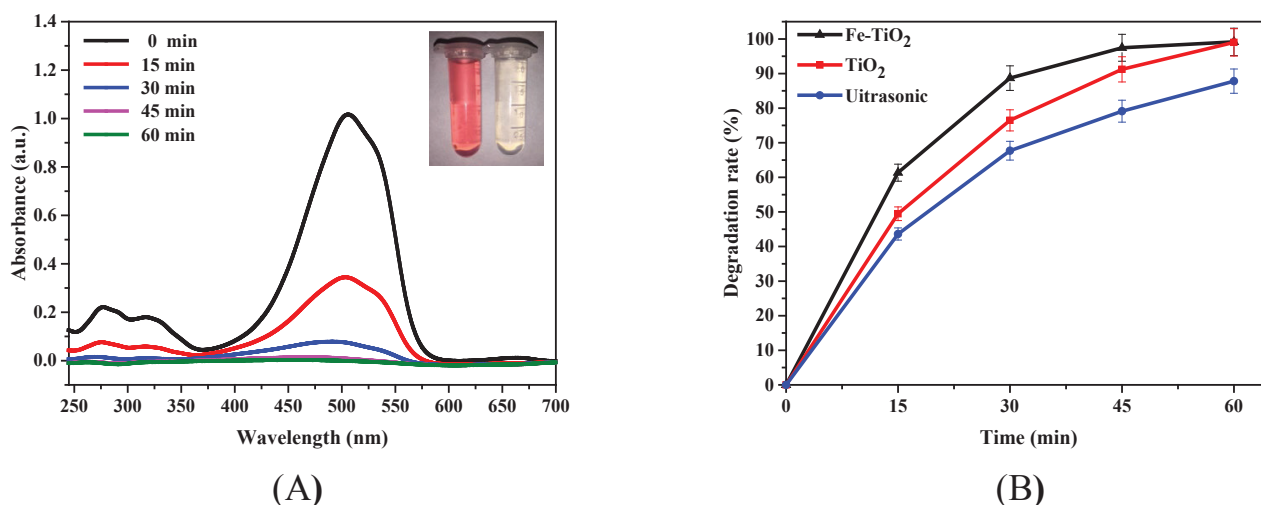
Figure 6: (A): Changes in the absorbance during the degradation of methyl orange. (B): Effect of time on sonocatalytic degradation of methyl orange. (Initial dye concentration = 10 mg/L, Catalyst loading = 0.5 g/L, Ultrasonic frequency = 40 kHz, pH= 3.0 Revolutions =500 r/min, Time=45 min).

under the action of nanoparticles, the reaction environment of ultrasonic catalytic degradation with the Fe-doped TiO_2 nanoparticles was not similar to that without the Fe-doped TiO_2 nanoparticles. In the absence of the Fe-doped TiO_2 nanoparticles, the degradation efficiency was gradually reduced under only ultrasonic. Because the increased concentration of MO, and the concentration of free radicals produced did not change under the experimental conditions. In the presence of the Fe-doped TiO_2 nanoparticles, the free radical product pathway changed. There may be a minimum effective reaction solution concentration in the catalytic reaction system. When the MO concentration is below that concentration value, the catalytic effect is not obvious. At the same time, the addition of catalyst may affect the reaction system of the original solution. Therefore, when adding nanoparticles, the degradation rate with methyl orange of 5 mg/L was lower than that of methyl orange with a concentration of 10 mg/L. The possible reason for the sonocatalytic degradation of simulated organic dye of methyl orange reduction could be attributed to the fact that when the initial concentration is increased, more reactant molecules are adsorbed on the surface of the ultrasonic catalyst, thus all the surface sites for the adsorption of hydroxyl ions are blocked and there is very low availability of the sites for the new generation of hydroxyl radicals. Consequently, the sonocatalytic degradation efficiency of methyl orange is decreased. At the same time, the high concentration of methyl orange solution is higher than that of the low concentration of methyl orange solution on the surface of the catalyst, which inhibits the efficiency of

the surface of the catalyst on the light and heat energies produced by ultrasonic cavitation. Therefore, the selection of a suitable initial concentration is necessary for the ultrasonic catalytic activity of any catalyst.

### 3.2.4 Effect of initial pH value

The effect of changing the initial pH value of methyl orange solution on sonocatalytic degradation was shown in Figure 7(C). In order to investigate the effect of pH value of methyl orange solution, five different pH value (initially at 3, 5, 7, 9 and 11) of methyl orange were selected, the suspension was prepared by mixing 10 mg/L of methyl orange solutions and 0.5 g/L TiO_2 nanoparticles for a reaction time of 45 min. It is found that the adsorption behavior of the catalyst had no obvious effect on the degradation rate under the ultrasonic and mechanical agitation at different pH values (data not shown). As can be seen, the sonocatalytic degradation efficiency is faster in an acidic media than in alkaline media and the most effective degradation rate was pH = 3. The methyl orange has a high concentration in the bubble interface in an acidic pH, so it was more vulnerable to the •OH radical attack. Acidic media accelerate degradation, this acceleration may be related to the hydrophobic character of the protonated negatively charged $-SO_3^-$ group in acidic media, which enhances its reactivity under ultrasound treatment. Moreover, the composition of methyl orange would change to the quinone type, which is unstable and easy to be destroyed under pH= 3.2, when the pH value is
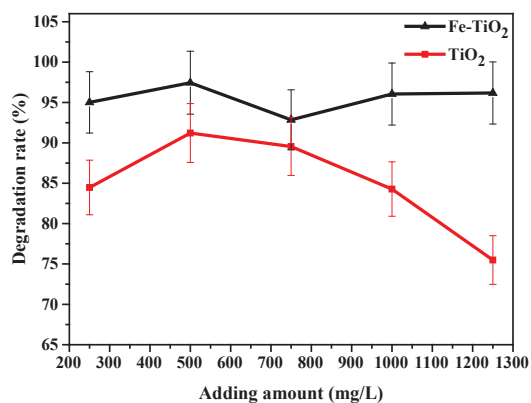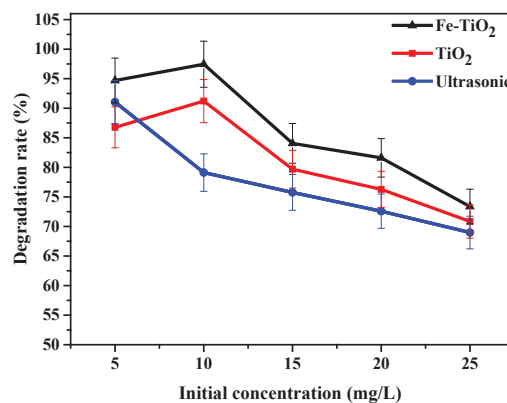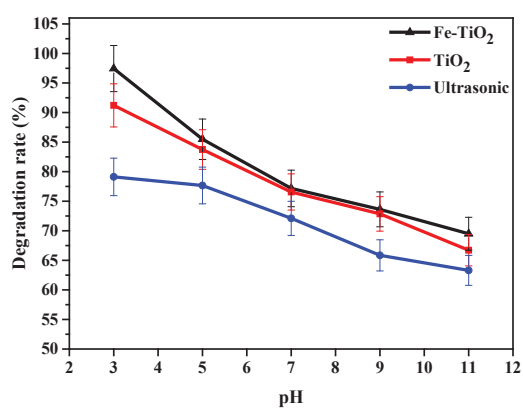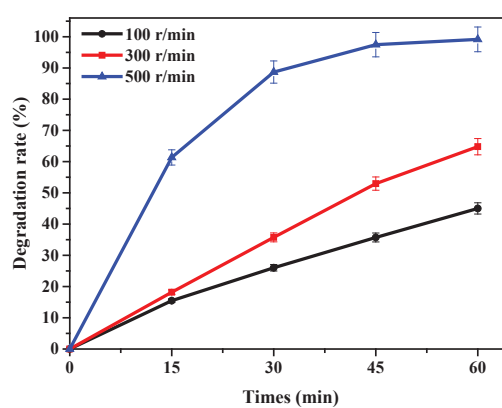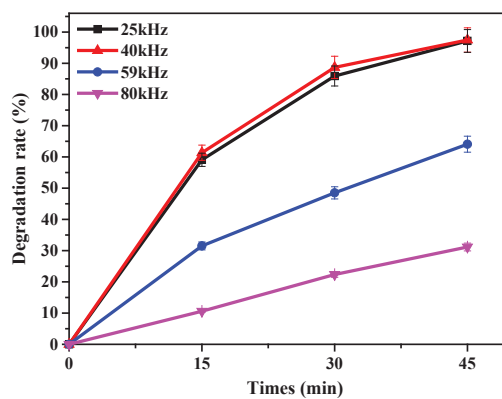
Figure 7: Effect of (A) TiO$_2$ added amount, (B) initial concentration, (C) pH, (D) revolutions per minute and (E) ultrasonic frequency on sonocatalytic degradation of methyl orange.

greater than 4.4, the azo bond is strong and difficult to be destroyed [4].

3.2.5 Effect of revolutions per minute

In order to overcome the problem that the solution in the container of the ultrasonic cleaning machine couldn't react violently, the experiment has explored a certain number of rotations to the suspension to be degraded. From Figure 7(D), it can be seen that the revolutions per minute of the mechanical agitator can be one of the very significant parameters for the degradation of MO. As shown in the figure, three different speeds (100, 300, and 500 rpm) were explored in this experiment. The range of revolutions per minute was selected during the experiment, because of the number of revolutions was greater than 500 rpm, the suspension would splash of the experimental flask so that it could not continue to experiment. Hence, the range of 100-500 rpm was chosen as the range for conducting the experiments.

Generally, the results show that the degradation rate increased with increasing revolutions of the mechanical agitator. The possible reason for the ultrasonic catalytic degradation of methyl orange reduction could be attributed to the fact that when the revolutions was increased, more reactant molecules were transferred on the surface of the Fe-doped modified TiO_2, thus all surface active sites were fully utilized and there was used immediately of the sites for the new generation of hydroxyl radicals, and then leave the active sites, the other molecules continue to react, effectively degrade the organic dye. Finally, when the degradation time was 45 min and the rotational speed is 500 rpm, the degradation rate has reached 97%. Therefore, the best number of revolutions for this test is 500 rpm.

3.2.6 Effect of ultrasonic vibration frequency

To study the effect of ultrasonic vibration frequency on ultrasonic catalytic degradation of methyl orange, we investigated four frequencies of 25, 40, 59, and 80 kHz. The results illustrated in Figure 7(E) shows that the overall trend of degradation rate was increased with the increase of irradiation time under the irradiation of four kinds of frequency ultrasound. The high degradation rate is gained from the ultrasonic radiation of low frequency, and the best choice of the frequency should be 40 kHz. The probable cause of this phenomenon is that the formation, growth, and rupture of cavitation bubbles in liquids

were easier to complete under the condition of stirring ultrasound. A large number of light and heat generated by the rupture of cavitation bubbles was transmitted to the surface of the nanoparticle catalyst, which greatly increases the degradation rate.

3.3 Effect of some other factors on the degradation rate

3.3.1 Effect of the sunlight and physical adsorption

The concentration decrease of the dye may also result from the photocatalytic degradation and physical adsorption by Fe-doped TiO_2. Thus, the reaction in the dark and the adsorption amount test of dye on TiO_2 is carried out. The result is shown in Figure 8(A). It is found that the reaction in the dark had no obvious effect on the degradation rate, the possible reason is that the effect of sunlight on the degradation rate is very small under the ultrasonic and mechanical agitation. Under the same strength of mechanical agitation, it is found that the adsorption amount test of dye on Fe-doped TiO_2 can be omitted. As is known to all, most of the dye adsorbed was immediately desorbed under the function of ultrasound with 10 min [4], thus, we neglected the effect of adsorption amount on the degradation rate in the experiment.

3.3.2 Effect of catalyst stability

The reusability of Fe-doped TiO_2 sonocatalytic removal of MO was also tested five times, and nanoparticles were treated by centrifugation to precipitate and dried in the drying oven at 85°C for 5 h. The result is shown in Figure 8(B). The sonocatalytic degradation rate was detected at 97.5% for the first time, and the degradation rate decreased slightly to 96.8% after six times. Therefore, it was confirmed that Fe-doped TiO_2 nanoparticles have an excellent stability and reusability under the ultrasonic and mechanical agitation.

3.4 Response surface optimization

From the above six experimental of ultrasonic degradation efficiency, it can be seen that the single factor of pH, time and rotation have no peak value. The best experimental results cannot be obtained through response surface analysis. So we got rid of these three single factors. The range of the experiment and the level of the variables
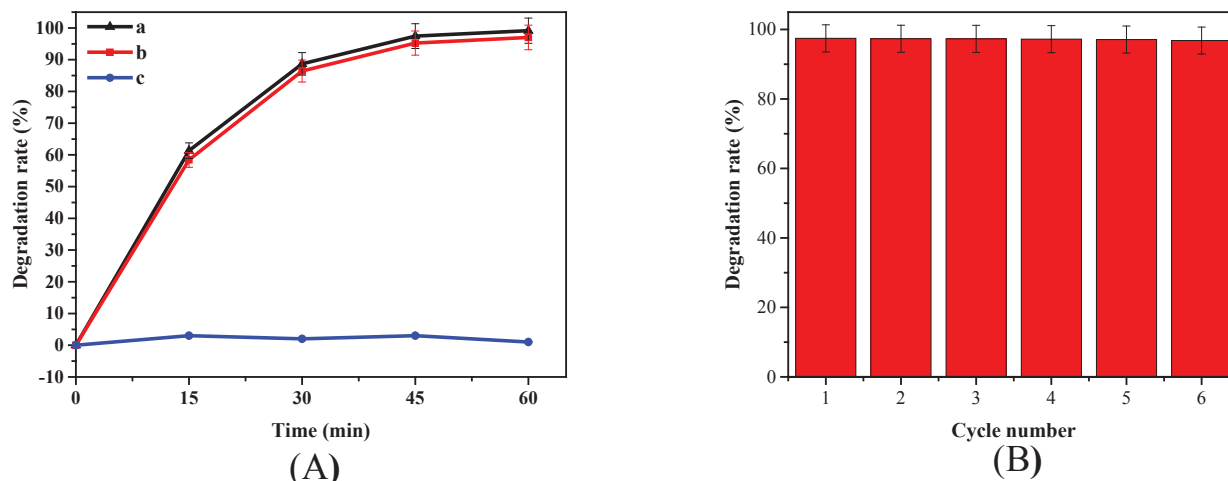
Figure 8: (A): Effect of the sunlight and physical adsorption on the degradation by Fe-doped TiO$_2$ powder (a: the reaction in the sunlight, b: the reaction in the dark, c: the adsorption amount test of dye on Fe-doped TiO$_2$). (B): Effect of sonocatalyst reusability on the sonocatalytic degradation of MO in aqueous solution.

Table 2: Experimental ranges and levels of the variables.

Variables	Symbol	Ranges and levels		
	x$_i$	-1	0	+1
Adding amount	X$_1$	250	500	750
Initial concentration	X$_2$	5	10	15
Ultrasonic frequency	X$_3$	25	40	59

(adding amount, initial concentration and ultrasonic frequency) are shown in Table 2 using the RSM technique. Combination of different factors in the experimental design and experimental and theoretical predicted values of methyl orange degradation rate are displayed in Table 3. The influence on the degradation rate of methyl orange by the adding amount, initial concentration and ultrasonic frequency is displayed in Figure 9.

From Figure 9, it can be seen that the response surface figure (3D) and contour plots of the sonocatalytic degradation of MO by Fe-doped modified TiO$_2$ powder catalyst as a function of these three single factors (adding amount, initial concentration and ultrasonic frequency). In Figure 9(A), the degradation rate of MO is obtained with a different adding amount and initial concentration at the ultrasonic frequency of 0 levels. It can be seen that the interactions of adding the amount and initial concentration are not significant. As can be seen from Figure 9(B), the increasing trend of the ultrasonic frequency is more obvious than that of the additive amount. Figure 9(C) displays results show the ultrasonic

vibration frequency has the obvious influence on the degradation rate. It is known that it is consistent with the single factor test.

By means of RSM of the obtained experimental data, a statistical model is established by a quadratic equation, and the best experimental conditions and the best degradation rate are obtained by the model analysis. The quadratic equation is as follows:

$$Y = -44.14 + 0.12X_1 + 9.35X_2 + 3.76X_3 - 8.6 \times 10^{-4}X_1X_2 +$$
$$+ 5.86 \times 10^{-4}X_1X_3 - 0.01X_2X_3 - 1.38 \times 10^{-4}X_1{}^2 - 0.46X_2{}^2 - 0.05X_3{}^2$$

The results of mathematical regression analysis model can be seen that the best conditions for ultrasonic catalytic degradation of the methyl orange obtained were: the initially added amount of catalyst = 490.50 mg/L, the initial concentration of methyl orange = 9.22 mg/L and ultrasonic frequency = 36.02 kHz.
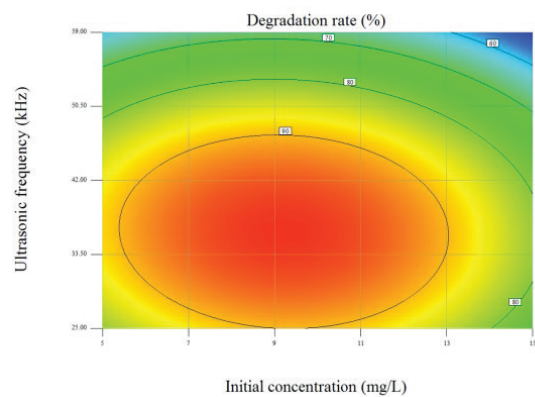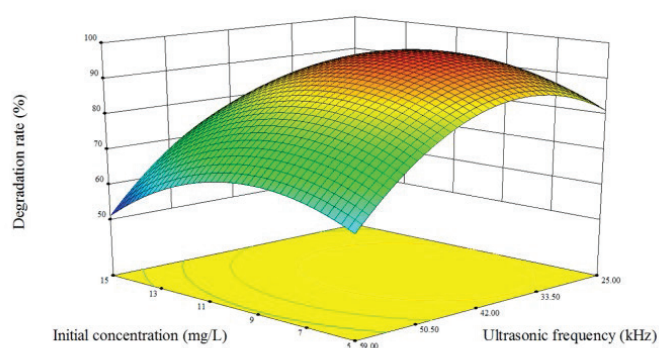
（A）
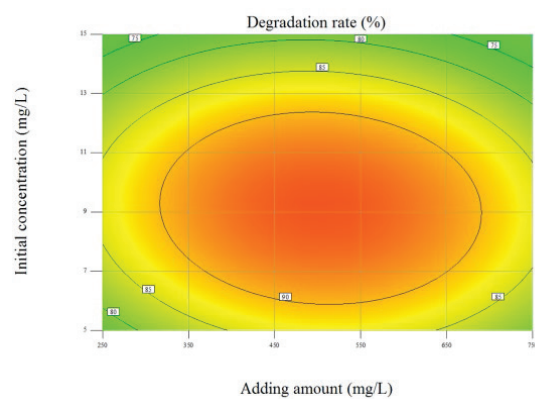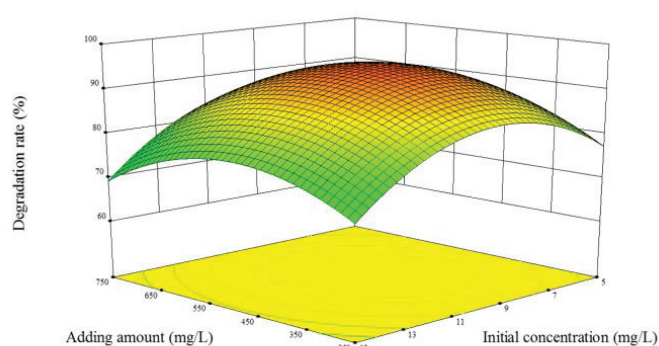
（B）
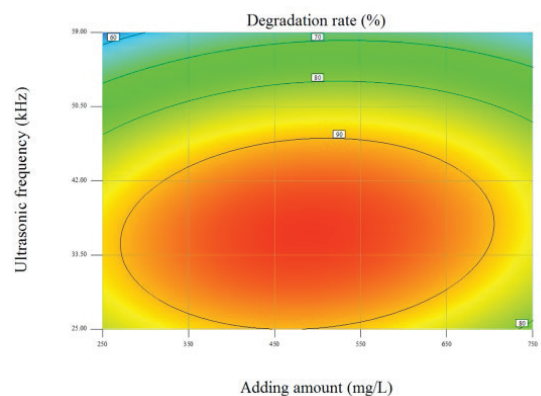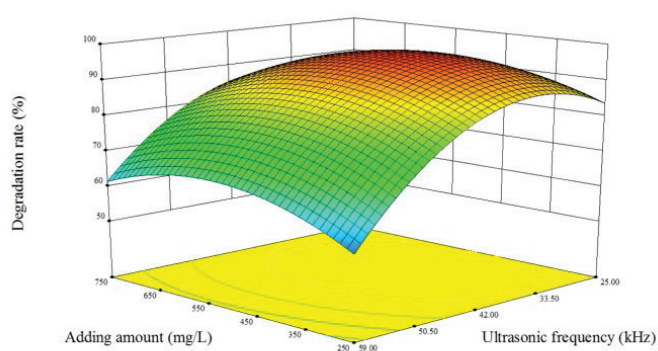
（C）

Figure 9: Response surface figure (3D) and contour plots of the sonocatalytic degradation of methylorange by Fe-doped TiO$_2$ powder catalyst as a function of (A) adding amount and initial concentration, (B) adding amount and ultrasonic frequency, (C) initial concentration and ultrasonic frequency.

Table 3: The 3-factor Box-Behnken experimental design and the results for degradation rate of methyl orange.

Run	Adding amount (mg/L)	Initial concentration (mg/L)	Ultrasonic frequency (kHz)	Degradation rate (%) Experimental	Predicted
1	750.00	10.00	59.00	62.09	61.47
2	250.00	5.00	40.00	78.41	78.50
3	500.00	10.00	40.00	97.35	95.58
4	750.00	5.00	40.00	77.14	80.15
5	750.00	10.00	25.00	81.06	78.77
6	500.00	10.00	40.00	92.67	95.58
7	500.00	15.00	59.00	50.32	51.02
8	750.00	15.00	40.00	70.33	70.24
9	500.00	10.00	40.00	98.89	95.58
10	500.00	15.00	25.00	73.08	75.48
11	250.00	10.00	59.00	54.47	56.42
12	500.00	5.00	59.00	63.24	61.21
13	500.00	10.00	40.00	93.88	95.58
14	500.00	10.00	40.00	95.12	95.58
15	250.00	10.00	25.00	82.71	83.67
16	500.00	5.00	25.00	82.37	81.31
17	250.00	15.00	40.00	75.90	72.90

3.5 Possible mechanism of the reaction

The ultrasonic degradation mechanism of MO dyes in Fe-doped modified TiO_2 nanoparticles is shown in Figure 10. The solution of the reaction produces cavitation bubbles under the action of ultrasonic radiation, and then the bubbles continue to absorb the sound energy in a very short time, the bubbles collapse and release the energy to cause ultrasonic cavitation phenomenon [31]. At the same time, single-bubble sonluminescence (SBSL) will appear, and a quite number of local "hot spots" with extremely high temperature and pressure [4]. The decomposition process of water molecules produced ·OH and ·H radicals, most of which occur on the surface of the catalyst.

The light and heat generated by ultrasonic cavitation can be excited rutile TiO_2 on the surface of nanoparticles [33]. Then, the electron-hole (e^- and h^+) pairs are constantly formed. On the one hand, the electrons on the surface of the catalyst are obtained by oxygen molecules, and a series of reactions follow and produce some active substances such as ·OH, $·O_2^-$ and H_2O_2 (Eqs. (2-4)). On the other hand, the electrons entered to anatase TiO_2. Finally, a lot of electrons are trapped by Fe^{3+} ions doped in anatase titanium dioxide (Eqs. (5) and (6)). Hence, a lot of oxygen is added to the reaction under the stirring of ultrasound. And the existence of Fe^{3+} ions in the catalyst accelerates the production of OH radicals. Table 4 shows the kinetic
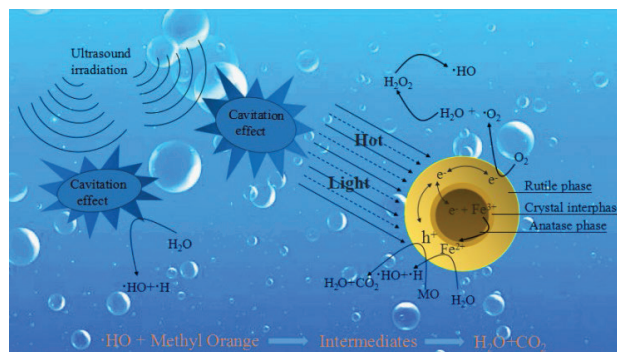

Figure 10: A schematic mechanism for the nanocatalysis of MO dye over Fe-doped TiO_2 nanoparticles (e^-: negative electron, h^+: positive hole, MO: Methyl Orange)

rate constant of these compounds with the specific ROSs [34]. This degradation mechanism was confirmed by the addition of ethanol in excess and a little NaCl (0.06mM), as hydroxyl radical scavenger, in which the degradation efficiency was suppressed (The data is shown in Figure 11). These results support the free radical attack pathway. So the ultrasonic catalytic activity is greatly improved under the conditions of Fe^{3+} ions doped in TiO_2 and stirring.

$$O_2 + e^- \rightarrow O_2^- \qquad (2)$$

$$·O_2^- + H_2O \rightarrow H_2O_2 \qquad (3)$$

Table 4: Kinetic rate constant of some organic and inorganic scavenging compounds with ·OH.

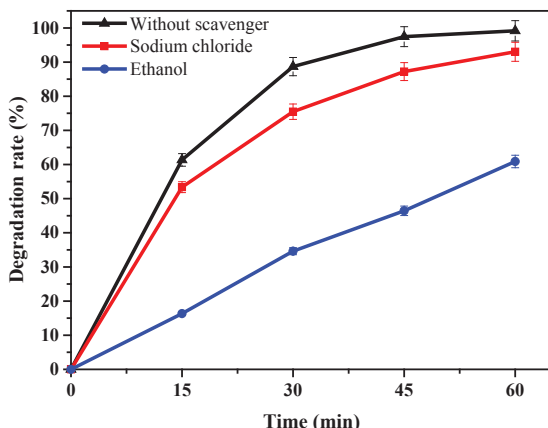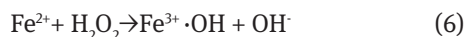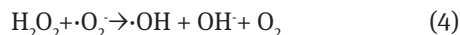| Scavengers	ROSs scavenged	k (M^{-1} s^{-1})
Ethanol	·OH	1.6×10^7
Cl$^-$	·OH	4.3×10^9

Figure 11: Effect of scavenging compounds on methyl orange sonocatalytic degradation rate (Ethanol = 0.6 M, Sodium chloride= 0.06 mM).

$$H_2O_2 + \cdot O_2^- \rightarrow \cdot OH + OH^- + O_2 \qquad (4)$$

$$Fe^{3+} + e^- \rightarrow Fe^{2+} \qquad (5)$$

$$Fe^{2+} + H_2O_2 \rightarrow Fe^{3+} \cdot OH + OH^- \qquad (6)$$

4 Conclusions

In this work, the modified TiO$_2$ and pure TiO$_2$ nanoparticles was prepared successfully by the sol-gel method and heat treatment. The XRD analysis reveals that the incorporation of Fe^{3+} ions affects the structure composition of the nanoparticles. The SEM and EDS analysis reveals that the incorporation of Fe^{3+} ions affects the sizes distribution of the nanoparticles. Ultrasonic radiation and mechanical agitation have a certain effect on the degradation of methyl orange. At the same time, we come to the conclusion that 0.5% Fe-doped modified TiO$_2$ powder has a higher degradation rate. The best parameters of degradation under agitated ultrasound by the analysis of the experimental data and response surface methods are obtained, such as initial added amount of catalytic powder

= 490.50 mg/L, pH = 3, 60 min, the initial concentration of methyl orange = 9.22 mg/L, ultrasonic vibration frequency of 36.02 kHz, and the revolutions per minute of 500 rpm. Meanwhile, the stirring rate of the suspension is also studied and found the degradation rate increased with increasing revolutions of the mechanical agitator. Sunlight has no significant effect on degradation rate, and Fe-doped TiO$_2$ nanoparticles have an excellent stability and reusability under the ultrasonic and mechanical agitation. The free radical attack causes degradation of organic dyes. The evidence shows that the combination of stirred ultrasonic catalysis and Fe^{3+} ion nanoparticles can effectively improve the degradation of organic pollutants.

Conflict of interest: Authors declare no conflict of interest.

References

[1] Sheshmani S., Ashori A., Hasanzadeh S., Removal of Acid Orange 7 from aqueous solution using magnetic graphene/chitosan: A promising nano-adsorbent, Int. J. Biol. Macromol., 2014, 68, 218-224.

[2] Zhang M., Yao Q., Lu C., Li Z., Wang W., Layered Double Hydroxide−Carbon Dot Composite: High-Performance Adsorbent for Removal of Anionic Organic Dye, ACS. Appl. Mater. Inter., 2014, 6, 20225-20233.

[3] Zhang Y., Zheng T.X., Hua Y.B., Guo X.L., Peng H.H., Zhang Y.X., et al., Delta manganese dioxide nanosheets decorated magnesium wire for the degradation of methyl orange, J. Colloid. Interf. Sci., 2017, 490, 226-232.

[4] Wang J., Guo B., Zhang X., Zhang Z., Han J., Wu J., Sonocatalytic degradation of methyl orange in the presence of TiO$_2$ catalysts and catalytic activity comparison of rutile and anatase, Ultrason. Sonochem., 2005, 12, 331-337.

[5] Santos A., Yustos P., Gomis S., Ruiz G., Garcia-Ochoa F., Generalized Kinetic Model for the Catalytic Wet Oxidation of Phenol Using Activated Carbon as the Catalyst, Ind. Eng. Chem. Res., 2005, 44, 3869-3878.

[6] Wang K.H., Hsieh Y.H., Chou M.Y., Chang C.Y., Photocatalytic degradation of 2-chloro and 2-nitrophenol by titanium dioxide suspensions in aqueous solution, Appl. Catal. B-Environ., 1999, 21, 1-8.

[7] Qi Y., Zhao L., Ojekunle Olusheyi Z., Tan X., Isolation and preliminary characterization of a 3-chlorobenzoate degrading bacteria, J. Environ. Sci. (China), 2007, 19, 332-337.

[8] Wang D., Bolton J.R., Hofmann R., Medium pressure UV combined with chlorine advanced oxidation for

trichloroethylene destruction in a model water, Water Res., 2012, 46, 4677-4686.

[9] Nikpassand M., Fekri L.Z., Farokhian P., An efficient and green synthesis of novel benzoxazole under ultrasound irradiation, Ultrason. Sonochem., 2016, 28, 341-345.

[10] Safaei-Ghomi J., Masoomi R., An efficient comparison of methods involving conventional, grinding and ultrasound conditions for the synthesis of fulleroisoxazolines, Ultrason. Sonochem., 2015, 23, 212-218.

[11] Nagargoje D., Mandhane P., Shingote S., Badadhe P., Gill C., Ultrasound assisted one pot synthesis of imidazole derivatives using diethyl bromophosphate as an oxidant, Ultrason. Sonochem., 2012, 19, 94-96.

[12] Zhang N., Zhang G., Chong S., Zhao H., Huang T., Zhu J., Ultrasonic impregnation of MnO_2/CeO_2 and its application in catalytic sono-degradation of methyl orange, J. Environ. Manage., 2018, 205, 134-141.

[13] Al-Juboori R.A., Aravinthan V., Yusaf T., Impact of pulsed ultrasound on bacteria reduction of natural waters, Ultrason. Sonochem., 2015, 27, 137-147.

[14] Lastre-Acosta A.M., Cruz-González G., Nuevas-Paz L., Jáuregui-Haza U.J, Teixeira A.C., Ultrasonic degradation of sulfadiazine in aqueous solutions, Environ. Sci. Pollut. R, 2015, 22, 918-925.

[15] Chong S., Zhang G., Wei Z., Zhang N., Huang T., Liu Y., Sonocatalytic degradation of diclofenac with FeCeOx particles in water, Ultrason. Sonochem., 2017, 34, 418-425.

[16] Khataee A., Karimi A., Hasanzadeh A., Joo S.W., Kinetic modeling of sonocatalytic performance of Gd-doped CdSe nanoparticles for degradation of Acid Blue 5, Ultrason. Sonochem., 2017, 39, 344-353.

[17] He L.L., Liu X.P., Wang Y.X., Wang Z.X., Yang Y.J., Gao Y.P., et al., Sonochemical degradation of methyl orange in the presence of Bi_2WO_6: Effect of operating parameters and the generated reactive oxygen species, Ultrason. Sonochem., 2016, 33, 90-98.

[18] Khataee A., Karimi A., Arefi-Oskoui S., Darvishi C.S.R., Hanifehpour Y., Soltani B., et al., Sonochemical synthesis of Pr-doped ZnO nanoparticles for sonocatalytic degradation of Acid Red 17, Ultrason. Sonochem., 2015, 22, 371-381.

[19] Wang J., Jiang Z., Zhang L., Kang P., Xie Y., Lv Y., et al., Sonocatalytic degradation of some dyestuffs and comparison of catalytic activities of nano-sized TiO_2, nano-sized ZnO and composite TiO_2/ZnO powders under ultrasonic irradiation, Ultrason. Sonochem., 2009, 16, 225-231.

[20] Abdullah A.Z., Ling P.Y., Heat treatment effects on the characteristics and sonocatalytic performance of TiO_2 in the degradation of organic dyes in aqueous solution, J. Hazard. Mater., 2010, 173, 159-167.

[21] Khataee A., Sheydaei M., Hassani A., Taseidifar M., Karaca S., Sonocatalytic removal of an organic dye using TiO_2/ Montmorillonite nanocomposite, Ultrason. Sonochem., 2015, 22, 404-411.

[22] Pang Y.L., Abdullah A.Z., Effect of low Fe^{3+} doping on characteristics, sonocatalytic activity and reusability of TiO_2 nanotubes catalysts for removal of Rhodamine B from water, J. Hazard. Mater., 2012, 235-236, 326-335.

[23] Santos R. S., Faria G. A., Giles C., Leite C. A., Barbosa H. S., Arruda M. A., et al., Iron insertion and hematite segregation on Fe-doped TiO_2 nanoparticles obtained from sol-gel and hydrothermal methods, ACS Appl. Mater. Inter., 2012, 4, 5555-5561.

[24] Caratto V., Locardi F., Alberti S., Villa S., Sanguineti E., Martinelli A., et al., Different sol–gel preparations of iron-doped TiO_2, nanoparticles: characterization, photocatalytic activity and cytotoxicity, J. Sol-Gel Sci. Techn., 2016, 80, 152-159.

[25] Zhou G., Wang W., Zheng B., Li Y., Preparation and photocatalytic properties of Fe^{3+}-doped TiO_2 nanoparticles, Eur. Chem. Bull, 2013, 2, 182-1045-1048.

[26] Dawber J.G., Fisher D.T., Warhurst P.R., The Metachromism of Methyl Orange with Electrolytes and Possible Salting-out, J. Chem. Soc. Faraday Tran.1, 1986, 82, 119-123.

[27] Kucukosmanoglu M., Gezici O., Ayar A., The adsorption behaviors of Methylene Blue and Methyl Orange in a diaminoethane sporopollenin-mediated column system, Sep. Purif. Technol., 2006, 52, 280-287.

[28] Dutta A., Dutta R.K., Fluorescence behavior of cis-methyl orange stabilized in cationic premicelles, Spectrochim. Acta A., 2014, 126, 270-279.

[29] Teng M., Qiao J., Li F., Bera P.K., Electrospun mesoporous carbon nanofibers produced from phenolic resin and their use in the adsorption of large dye molecules, Carbon, 2012, 50, 2877-2886.

[30] Huang R., Liu Q., Huo J., Yang B., Adsorption of methyl orange onto protonated crosslinked chitosan, Arab. J. Chem., 2017, 10, 24-32.

[31] Soltani R.D.C., Jorfi S., Ramezani H., Purfadakari S., Ultrasonically induced ZnO−biosilica nanocomposite for degradation of a textile dye in aqueous phase, Ultrason. Sonochem., 2016, 28, 69-78.

[32] Tabasideh S., Maleki A, Shahmoradi B., Ghahremani E., Mckay G., Sonophotocatalytic degradation of diazinon in aqueous solution using iron-doped TiO_2 nanoparticles, Sep. Purif. Technol., 2017, 189, 186-192.

[33] Wang J., Sun W., Zhang Z., Jiang Z., Wang X., Xu R., et al., Preparation of Fe-doped mixed crystal TiO_2 catalyst and investigation of its sonocatalytic activity during degradation of azo fuchsine under ultrasonic irradiation, J. Colloid. Interf. Sci., 2008, 320, 202-209.

[34] Khataee A., Honarnezhad R., Fathinia M., Degradation of sodium isopropyl xanthate from aqueous solution using sonocatalytic process in the presence of chalcocite nanoparticles: Insights into the degradation mechanism and phytotoxicity impacts, J. Environ. Manage., 2018, 211, 225-237.